Gene Therapy (2016) **23**, 26–37
© 2016 Macmillan Publishers Limited All rights reserved 0969-7128/16
www.nature.com/gt

ORIGINAL ARTICLE

Intradermal delivery of DNA encoding HCV NS3 and perforin elicits robust cell-mediated immunity in mice and pigs

B Grubor-Bauk[1,3], W Yu[1,3,4], D Wijesundara[1], J Gummow[1], T Garrod[1,5], AJ Brennan[2], I Voskoboinik[2] and EJ Gowans[1]

Currently, no vaccine is available against hepatitis C virus (HCV), and although DNA vaccines have considerable potential, this has not been realised. Previously, the efficacy of DNA vaccines for human immunodeficiency virus (HIV) and HCV was shown to be enhanced by including the gene for a cytolytic protein, viz. perforin. In this study, we examined the mechanism of cell death by this bicistronic DNA vaccine, which encoded the HCV non-structural protein 3 (NS3) under the control of the CMV promoter and perforin is controlled by the SV40 promoter. Compared with a canonical DNA vaccine and a bicistronic DNA vaccine encoding NS3 and the proapoptotic gene *NSP4*, the perforin-containing vaccine elicited enhanced cell-mediated immune responses against the NS3 protein in vaccinated mice and pigs, as determined by ELISpot and intracellular cytokine staining, whereas a mouse challenge model suggested that the immunity was $CD8^+$ T-cell-dependent. The results of the study showed that the inclusion of perforin in the DNA vaccine altered the fate of NS3-positive cells from apoptosis to necrosis, and this resulted in more robust immune responses in mice and pigs, the latter of which represents an accepted large animal model in which to test vaccine efficacy.

Gene Therapy (2016) **23,** 26–37; doi:10.1038/gt.2015.86

INTRODUCTION

Hepatitis C virus (HCV) is a major cause of chronic liver disease and as such represents a global health problem, as an estimated ~200 million individuals are infected with HCV worldwide.[1] Individuals infected with HCV genotype 1 can be treated successfully with pegylated interferon-α (IFN-α)/ribavirin combined with a direct-acting anti-viral agent, teleprevir or boceprevir. Although additional direct-acting anti-viral agent, which are effective against multiple genotypes, are also available, the high cost of therapy emphasises the need for the development of novel strategies for vaccination against HCV infection.[2] Currently, no vaccine is available against HCV, but several candidates have been evaluated in phase I and II clinical trials.[3,4]

Acute hepatitis C infection is associated with spontaneous clearance in ~25% of infected individuals.[5] It has been shown that cell-mediated immunity (CMI), particularly to more genetically conserved non-structural (NS) proteins, such as NS3, has an important role in virus clearance.[6] NS protein 3 (NS3) is a highly conserved, bifunctional protein with a serine protease in the N terminus and an RNA helicase in the C terminus.[7] It represents a promising target for immunisation, because NS3-specific $CD8^+$ and $CD4^+$ T-cell responses have been described as markers of viral clearance both in humans and chimpanzees.[8–12]

To date, the potential of DNA vaccines has not been realised mainly because of their suboptimal delivery, poor antigen expression and the lack of a localised inflammatory response, all essential for antigen presentation and an effective immune response to the immunogens.[13,14]

To overcome the issues of poor DNA vaccine delivery, we chose intradermal delivery rather than the more commonly used intramuscular or subcutaneous routes, as evidence suggests that the delivery of DNA is more effective via the intradermal route, as the dermis/epidermis contain a higher frequency of different subsets of antigen-presenting cells (APCs), including dendritic cells (DCs), compared with the muscle tissue or subcutaneous fat.[15,16] Priming of naive T cells via antigen-loaded DCs is the primary aim of vaccination. Therefore, a successful DNA vaccine must directly target DCs and/or otherwise direct the antigen to cross-presenting DCs.[17]

As the non-cytolytic nature of DNA vaccination was proposed to be an additional contributing factor to its inefficiency, to combat this we showed that coexpression of an immunogen and the cytolytic protein, perforin (PRF), led to a non-apoptotic cell death and an increase in the immunogenicity of the human immunodeficiency virus-1 (HIV-1) Gag protein, the model antigen luciferase or HCV proteins after intradermal DNA vaccination.[18–20] PRF, a 67-kDa multidomain protein, upon degranulation, inserts itself into the plasma membrane of the target cell, forming a pore.[21,22] The effect of PRF was dependent on the level of antigen expression and the timing of cell death after expression of the immunogen. We also showed that the induction of cell death not only increased the immunogenicity of the Gag protein but importantly it resulted in increased protection against challenge with EcoHIV, a chimeric HIV that replicates in mice.[18]

The mechanism responsible for this increase in immunogenicity is thought to result from PRF-induced necrotic death of vaccine-targeted cells in the dermis followed by release of the endogenous immunogen and damage-associated molecular patterns (DAMPs), recognised as effective natural adjuvants.[23] The immunogen is then taken up by the DCs for cross-presentation,[24,25] resulting in

[1]Virology Laboratory, Discipline of Surgery, University of Adelaide and Basil Hetzel Institute for Translational Medicine, Adelaide, SA, Australia and [2]Killer Cell Biology Laboratory, Cancer Immunology Research, Peter MacCallum Cancer Centre, Melbourne, VIC, Australia. Correspondence: Dr B Grubor-Bauk, Virology Laboratory, Discipline of Surgery University of Adelaide and Basil Hetzel Institute for Translational Medicine, 37A Woodville Road, Adelaide 5011, SA, Australia.
E-mail: branka.grubor@adelaide.edu.au
[3]These authors contributed equally to this work.
[4]Current address: Experimental Therapeutics Laboratory, University of South Australia, Adelaide, SA, Australia.
[5]Current address: Royal Australasian College of Surgeons, North Adelaide, SA, Australia.
Received 16 December 2014; revised 22 July 2015; accepted 29 July 2015; accepted article preview online 11 August 2015; advance online publication, 1 October 2015

an accelerated, more robust CMI and increased protection against viral challenge compared with canonical DNA vaccines.

To clarify the mechanism behind the adjuvant effect of PRF-related cell death, we developed a DNA vaccine encoding the HCV NS3 protein and PRF and compared the effect of the NS3 PRF DNA vaccination to that of a DNA vaccine encoding NS3 and a well-defined proapoptotic protein, the rotavirus NS protein 4 (NSP4).[26] NSP4 is a 175-amino-acid protein with a fundamental role in rotavirus morphogenesis and pathogenesis.[27] Previous studies have reported that NSP4 exerts its proapoptotic effect by disruption of mitochondrial membrane potential and caspase activation, eliciting an intrinsic apoptotic pathway.[26] Therefore, it is an excellent candidate against which to compare the immunogenicity of NS3 coexpressed with PRF.

Although many DNA vaccine studies, including HCV DNA vaccine studies, have been performed in mice,[28–31] to our knowledge only one, to examine the immune response to a secreted form of the envelope glycoprotein E2, has been tested in preclinical studies in pigs,[32] a recognised large animal model in which to test vaccine immunogenicity before human clinical trials.[33] Thus, in this study, we aimed to clarify the mechanism of PRF-induced cell death and to compare the efficacy of our DNA vaccine in mice and pigs with that of a canonical DNA vaccine to generate data that will be critical for future human clinical trials.

RESULTS

PRF-induced cell death *in vitro*

DNA vaccines were constructed in pVAX (Thermo Fisher Scientific Inc., Scoresby, VIC, Australia), which has been optimised for use as a DNA vaccine (Figure 1a). Wild-type PRF is efficiently exported into the lysosomes/secretory granules, where it is safely stored until its release from the cell. In contrast, deletion of an unstructured C-terminal dodecapeptide of PRF results in its retention in the endoplasmic reticulum, without having any effect on the cytolytic function.[22,34] There, at the natural pH and elevated calcium concentrations, PRF becomes cytotoxic and kills the host cell, and it is this truncated from of PRF that was encoded in all of our DNA vaccines.[34] For this study, we constructed pVAX-NS3, pVAX-NS3-PRF and pVAX-NS3-NSP4 (Figure 1a) as bicistronic vectors, in which the upstream cistron (NS3) is controlled by the CMV promoter and the downstream cistron (NSP4 or PRF) is controlled by the SV40 promoter (Figure 1a). We have previously demonstrated that the SV40 promoter is ~10-fold weaker compared with the CMV promoter,[18] consistent with a previous study.[35] A plasmid in which PRF expression was controlled by the more efficient CMV promoter (pCMV-PRF) was included as a control.

The expression of NS3 was confirmed by western blot analysis of human kidney embryo 293T (HEK293T) cells transiently transfected with pVAX-NS3 or pVAX-NS3-PRF (Figure 1b), whereas PRF expression was confirmed by immunofluorescence to

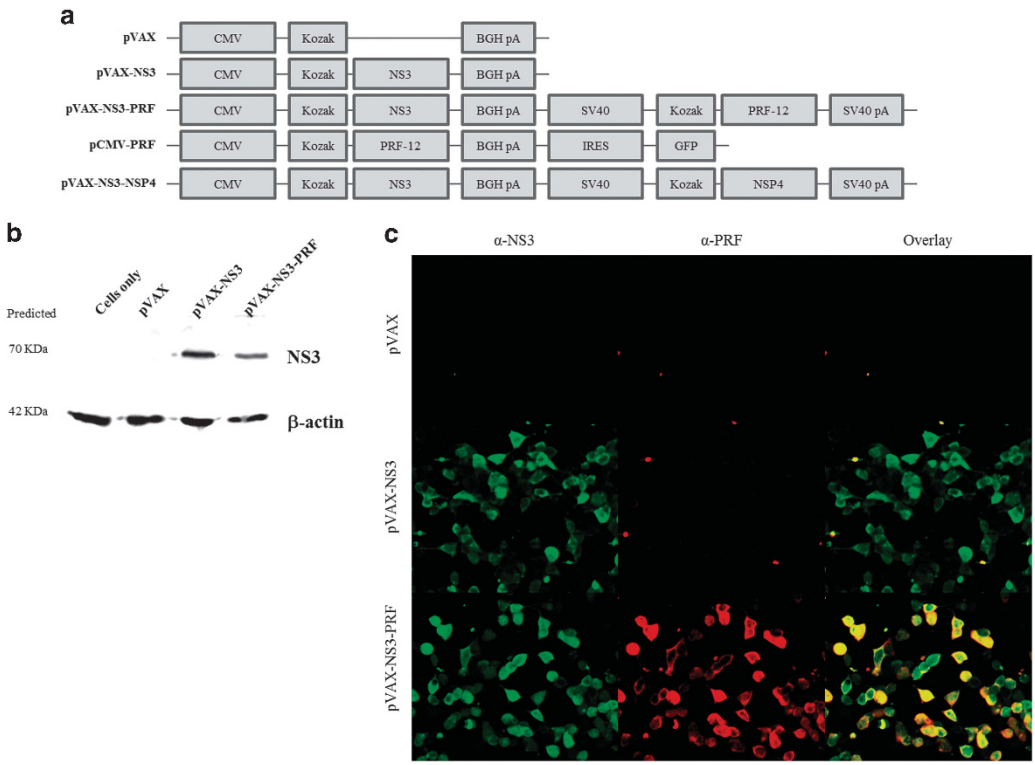

Figure 1. DNA constructs and protein expression. (**a**) Schematic diagram of DNA plasmids. pVAX-NS3 (4.9 kb) and the bicistronic pVAX-NS3-PRF (7.4 kb) and pVAX-NS3-NSP4 plasmids (6.5 kb) were based on the control plasmid pVAX (3 kb). HCV NS3 (g1b) was cloned into the multiple cloning site with a Kozak sequence for enhanced mammalian expression under the control of the CMV promoter, and flanked by the bovine growth hormone polyadenylation (BGH pA) site for the termination of transcription. In the bicistronic pVAX-NS3-PRF construct, the expression of the cytolytic gene *PRF* was under the control of SV40 promoter and was flanked by a downstream SV40 pA sequence. Expression of the rotavirus NSP4 protein was controlled in the same manner in the pVAX-NS3-NSP4 construct. pCMV-PRF (6.9 kb) containing the C-terminal truncated *PRF* gene (6.9 kb) was created on the pIRES-GFP backbone (Clontech, Mountain View, CA, USA) with gene expression driven by the CMV promoter. (**b**) Cell lysates from HEK293 T cells transfected with DNA encoding the NS3 were examined by western blot and probed with anti-NS3 antibody, with β-actin as a loading control. The blot is representative of three independent experiments. (**c**) Immunofluorescent staining of HEK293 T cells transfected with pVAX, pVAX-NS3 or pVAX-NS3-PRF. At 48 h after transfection, the cells were fixed and permeabilised, and the expression of NS3 and PRF was detected by immunofluorescence as described in the Materials and methods section.

© 2016 Macmillan Publishers Limited

emphasise that it colocalised with the NS3 protein (Figure 1c). Although our previous studies reported that cell death resulting from the expression of PRF resulted in increased responses to the immunogen, the actual mechanism of cell death was not determined.[18,20] To address this question, HEK293T cells were transfected with the respective DNA constructs and cell death was examined in a lactate dehydrogenase (LDH) release assay. The results of this experiment showed that pVAX-NS3-PRF-transfected cells showed increased death compared with pVAX-NS3-transfected cells (Figures 2a and b). Cell death resulting from expression of PRF from the SV40 promoter (pVAX-NS3-PRF) was ~40–50% of that from pCMV-PRF at 24–48 h after transfection, as expected since the CMV promoter was more efficient.[18] In contrast, cells treated by doxorubicin, a known inducer of apoptosis,[36] failed to show any significant release of LDH, as LDH is only released much later, once the cell membrane ruptures during secondary necrosis.[37,38] Thus, the LDH assay suggested that necrosis was the mechanism of cell death.

To further define the PRF-induced mechanism of cell death, HEK293T cells were transfected with the various DNA constructs and treated with necrostatin-1 (10 μM) or z-VAD-FMK (50 μmol l^{-1}). LDH release was measured 48 h after transfection (Figure 2c). Necrostatin-1, an inhibitor of the enzymatic activity of receptor-interacting protein kinase 1, is thought to be an inhibitor of receptor-interacting protein 1 (RIP1)/RIP-mediated caspase-independent necrosis,[39,40] whereas z-VAD-FMK is a widely used broad-spectrum caspase inhibitor. Necrostatin-1 significantly reduced LDH release from HEK293 cells transfected with pVAX-NS3-PRF or pCMV-PRF but not pVAX-NS3, suggesting that RIP1/RIP3 is responsible for the LDH release, and thus RIP/RIP3 mediated necrosis in these cells (Figure 2c). The inhibition by necrostatin-1 was incomplete most likely because of incomplete inhibition of the kinase in intact, untransfected cells. Treatment of pCMV-PRF-transfected cells with z-VAD-FMK had no significant effect on LDH release (Figure 2c). Interestingly, treatment of pVAX-NS3-PRF-transfected cells with z-VAD-FMK also resulted in a significant reduction in LDH release, as did the treatment of pVAX-NS3-transfected cells, whereas, as noted above, necrostatin-1 had no significant effect on LDH release from pVAX-NS3-transfected cells (Figure 2c). This is consistent with a previous study, which showed that overexpression of HCV NS3 and its precursor NS2/NS3 in mammalian cells led to apoptosis and activation of caspases.[41] Thus, the outcome of cells transfected with pVAX-NS3-PRF reflects the balance of NS3-induced apoptosis and PRF-mediated necrosis.

This was further investigated with a DEVD-caspase activity assay, in which HEK293 T-transfected cells were cultured in the presence or absence of z-VAD-FMK and caspase activity was assayed 48 h after transfection (Figure 2d). The amino-acid sequence Asp-Glu-Val-Asp (DEVD) corresponds to a sequence within PARP1 (poly(ADP-ribose) polymerase 1), a DNA repair enzyme. The DEVD sequence is cleaved by caspase-3 during apoptotic cell death. Consistent with the above data, pVAX-NS3-transfected cells showed higher caspase activity compared with pVAX-NS3-PRF cells. Caspase activity was inhibited by zVAD-FMK in doxorubicin-treated or pVAX-NS3-transfected cells, whereas

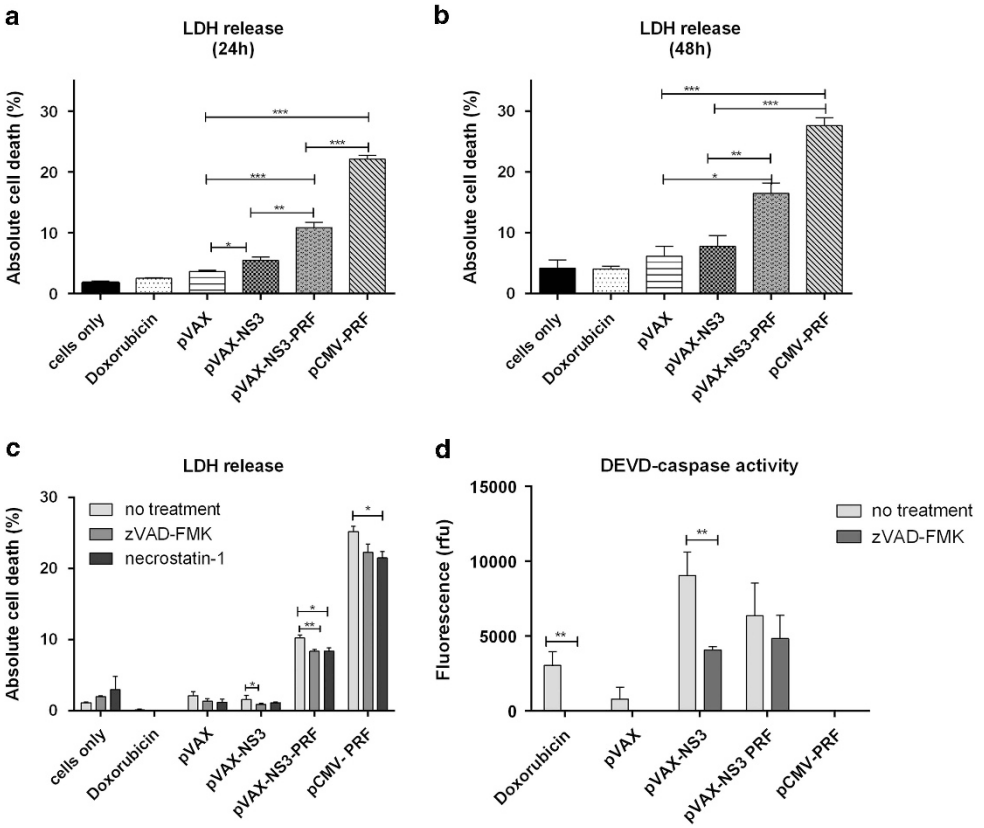

Figure 2. LDH assay of cell death and DEVD-caspase activity. HEK293T cells were transfected with 200ng of plasmid DNA in a 96-well plate or treated with 2 μM doxorubicin. LDH release was measured in the cell supernatant at 24 h (**a**) and 48 h after transfection (**b**). HEK293T cells were also transfected in the presence of necrostatin-1 and z-VAD-FMK inhibitors and LDH release was measured 48 h later (**c**). The results are presented as the mean percentage of cell death ± s.e.m based on the 100% lysis control. Transfected HEK293T cells were also cultured in the presence of z-VAD-FMK, and DEVD-caspase activity was measured in all samples (**d**). Data represent mean percentage of the fluorescence unit relative to caspase activity (**d**). *$P < 0.05$, **$P < 0.01$ and ***$P < 0.001$.

© 2016 Macmillan Publishers Limited

caspase activity was undetected in pCMV-PRF- transfected cells. Z-VAD-FMK had no significant effect on caspase activity in pVAX-NS3-PRF-transfected cells, and thus increased death of pVAX-NS3-PRF-transfected cells was associated with low caspase activity, consistent with non-apoptotic cell death.

Collectively, our findings indicate that pVAX-NS3-PRF-transfected cells predominantly undergo necrotic cell death.

To further elucidate the mechanism of cell death induced by PRF, we used the Huh-7 cell line as an alternative epithelial cell line, transfected these cells with the different DNA vaccine constructs and then examined the cells by conventional Annexin V and propidium iodide (PI) staining (Figure 3a). This experiment showed that 4.23% of the cells only control and 6.24% of the LTX control cells were PI^+, whereas 5.75% of the pVAX-NS3-PRF-transfected cells and 7.48% of the pVAX-NS3-transfected cells were PI^+. Thus, based on PI^+ staining, the cells failed to show evidence of necrosis resulting from expression of NS3 or PRF. In contrast, the proportion of cells that were Annexin V^+ after transfection was 9.62% and 11.56% in the cells only control and LTX control, respectively, whereas 18.08% of the pVAX-NS3-transfected cells and 28.46% of the pVAX-NS3-PRF-transfected cells were Annexin V^+ (Figure 3a). Thus, although release of LDH and the caspase-3 inhibition studies suggested that expression of NS3+PRF-induced non-apoptotic (necrotic) cell death, Annexin V and PI staining suggested that NS3 *per se* induced apoptosis, which is exaggerated by PRF coexpression. However, recent studies have detected phosphatidylserine exposure by Annexin V staining in non-apoptotic cell death,[42,43] and phosphatidylserine exposure is no longer considered to be an unambiguous marker of apoptosis.[44]

These apparently discrepant results were clarified by western blot detection of cytokeratin 18 (CK18) (Figure 3b), which is expressed in single layer epithelial tissues and is cleaved by activated caspases 3, 7 and 9 during apoptosis.[45–47] We examined the cleavage of CK18 by western blot to unambiguously identify apoptotic cells. We compared the expression and cleavage of

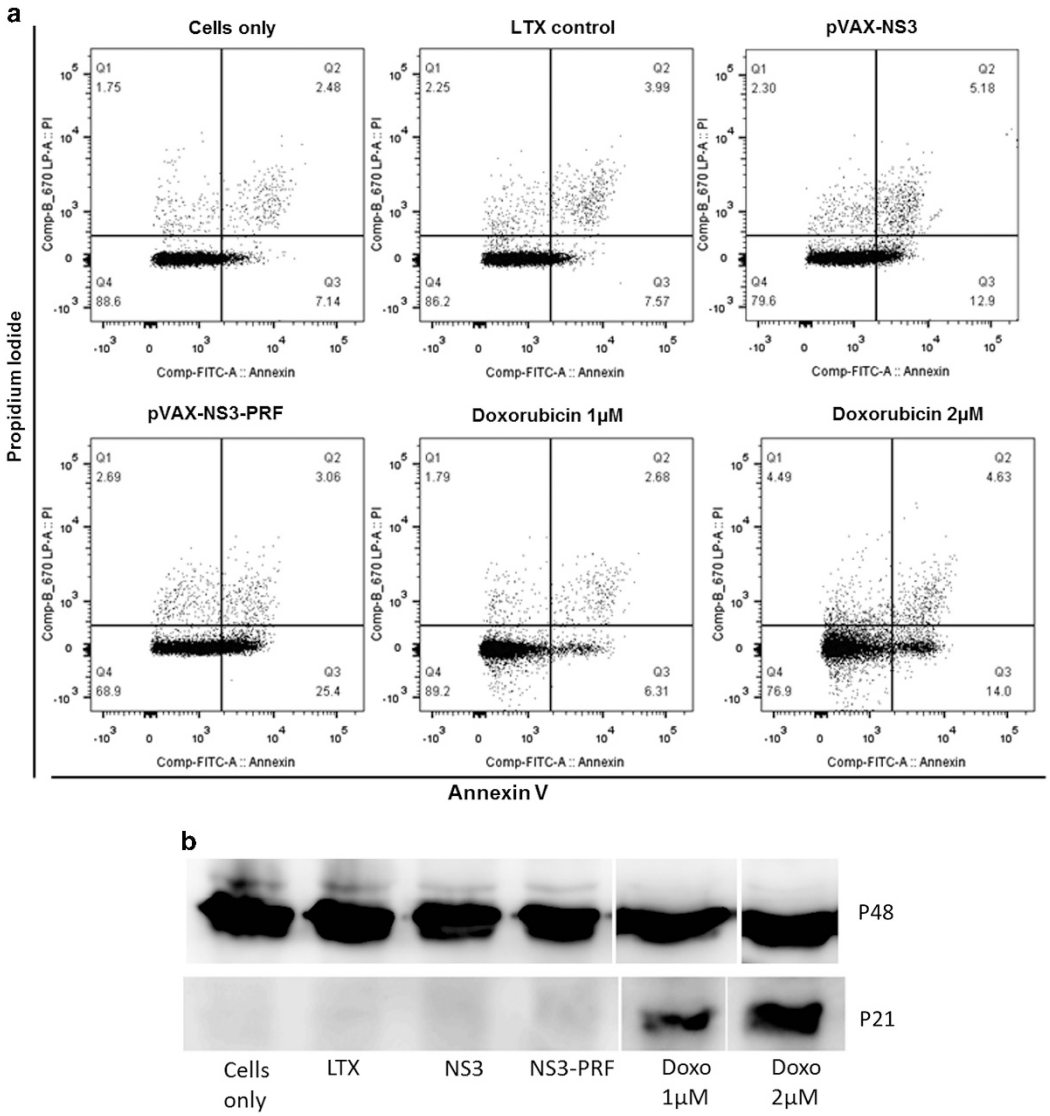

Figure 3. Expression of NS3-PRF results in non-apoptotic cell death. (**a**) Huh-7 cells were transfected with plasmid DNA or treated with 1 or 2 μM doxorubicin. Cell death was subsequently analysed by flow cytometry for PI and Annexin V staining at 48 h after transfection. (**b**) Western blot to detect the 21 kDa fragment of cytokeratin 18 in Huh-7 cells transfected with plasmid DNA or treated with doxorubicin. P48 is the full-length cytokeratin 18, which serves as a loading control. The protein content in the lysates was quantified by a BCA Kit (Thermo Fisher Scientific Inc.) and 84 μg of each sample was loaded for sodium dodecyl sulphate-polyacrylamide gel electrophoresis (SDS-PAGE) analysis and western blotting.

© 2016 Macmillan Publishers Limited

CK18 in Huh-7 cells, which were transfected with pVAX-NS3 or pVAX-NS3-PRF, with that resulting from the action of doxorubicin. The results of this experiment showed that CK18 was cleaved to result in a P21 cleavage product in the doxorubicin-treated cells, in a dose-dependent manner (Figure 3b, lanes 5 and 6). In contrast, cells transfected with pVAX-NS3 or pVAX-NS3-PRF showed no such product (Figure 3c, lanes 3 and 4). As the proportion of Annexin V^+ cells in the 2 μM doxorubicin-treated cells and the pVAX-NS3-transfected cells was very similar (18.63% and 18.08%, respectively) (Figures 3a and b), this provides a clear evidence that the mechanism of cell death differs in these two populations. Furthermore, as 28.46% of the pVAX-NS3-PRF-transfected cells were Annexin V^+, one might expect CK18 cleavage to be readily detected in this population, but this was not the case. Moreover, as the LTX reagent itself resulted in the death of 11.56% of cells, specific cell death resulting from expression of NS3 was determined to be 6.52% (18.08 – 11.56), whereas that resulting from NS3 and PRF expression was 16.90% (28.46 – 11.56), showing that NS3 and PRF expression resulted in a 2.6-fold increase in non-apoptotic cell death relative to NS3 expression alone. Thus, the expression of NS3 and PRF results in cell death by a non-apoptotic mechanism, which most likely occurs by necrosis that is mediated by RIP1 kinase activity.

Coexpression of PRF increased the NS3-specific response in mice

We then examined the efficacy of the DNA vaccine in mice to determine if the inclusion of PRF improved the cell-mediated immune response to NS3. Four groups of mice were vaccinated via the intradermal route with pVAX, pVAX-NS3, pVAX-NS3-PRF or pVAX-NS3-NSP4, respectively, as described in the Materials and methods section. Splenocytes were harvested 10 days after vaccination and restimulated with pools of overlapping peptides representing the complete NS3 protein (pools 1–3 as shown in Figures 4a and c) or with peptides pool covering two H-2^b (C57BL/6) immunodominant $CD8^+$ T-cell epitopes identified previously in an ELISpot[48] (Figure 4d). Compared with the control group that received the pVAX plasmid, the pVAX-NS3-immunised group showed an NS3-specific IFN-γ response to peptides in all three pools and to the immunodominant epitopes, although only the responses to pool 3 and the $CD8^+$ immunodominant epitopes were significantly higher compared with the background responses observed in pVAX-vaccinated mice. In contrast, the NS3-specific IFN-γ responses in the pVAX-NS3-PRF-vaccinated group showed a statistically significant increase in all peptide pools compared with the responses in the pVAX-vaccinated group (Figure 4). Furthermore, the responses to peptide pools 2 and 3 and the $CD8^+$ T-cell epitope pool were significantly higher in the pVAX-NS3-PRF-vaccinated group compared with those in the pVAX-NS3-vaccinated group. pVAX-NS3-PRF-vaccinated mice showed significantly higher NS3-specific responses in pool 1 compared with those observed for pVAX, and as this pool contains none of the immunodominant NS3 peptides, this represents a broadening of the immune response to nondominant epitopes.

We felt it was important to compare the effect of the inclusion of the proapoptotic rotavirus NSP4 protein on the immunogenicity

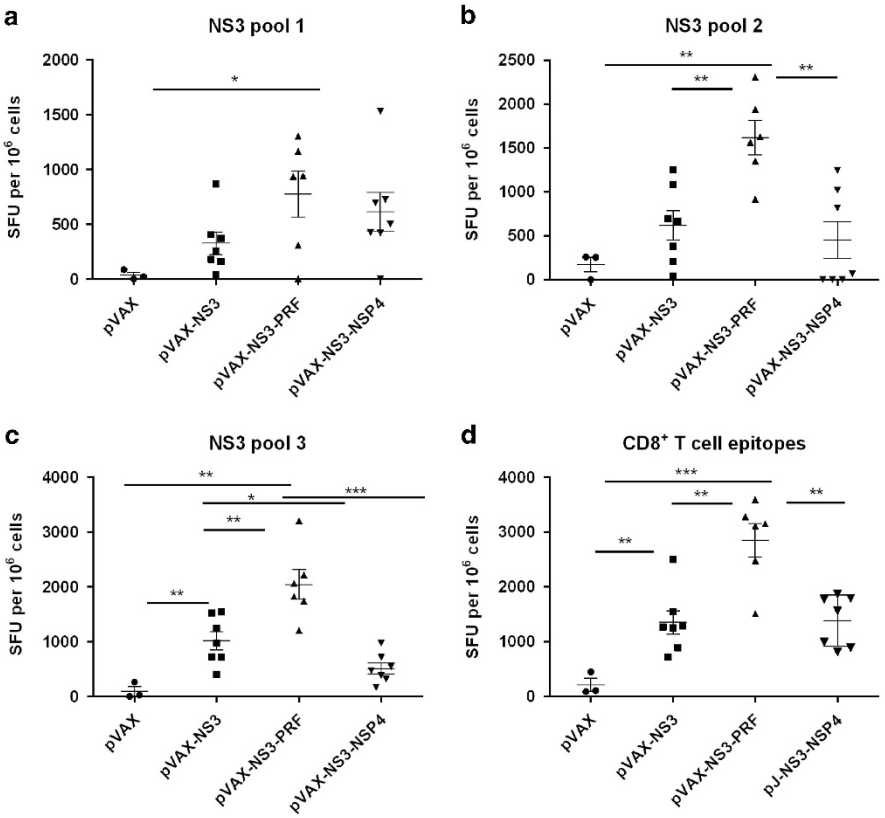

Figure 4. Immunisation with a DNA vaccine encoding HCV NS3 and PRF elicits strong NS3-specific CMI in mice. C57BL/6 mice were immunised (intradermally) three times with 50 μg of DNA (pVAX $n=7$, pVAX-NS3 $n=7$, pVAX-NS3-PRF $n=6$ or pVAX-NS3-NSP4 $n=7$) at 2-week intervals. NS3-specific T-cell responses were measured by IFN-γ production in an ELISpot assay. Splenocytes from vaccinated animals were restimulated with three different pools of overlapping peptides covering the complete NS3 protein (pools 1–3 as shown in **a**–**c**), or with a pool of H-2^b (C57BL/6) $CD8^+$ T-cell NS3 immunodominant epitopes. Data represent mean spot-forming units (SFU) per 10^6 splenocytes (± s.e.m). $^*P<0.05$, $^{**}P<0.01$ and $^{***}P<0.001$.

© 2016 Macmillan Publishers Limited

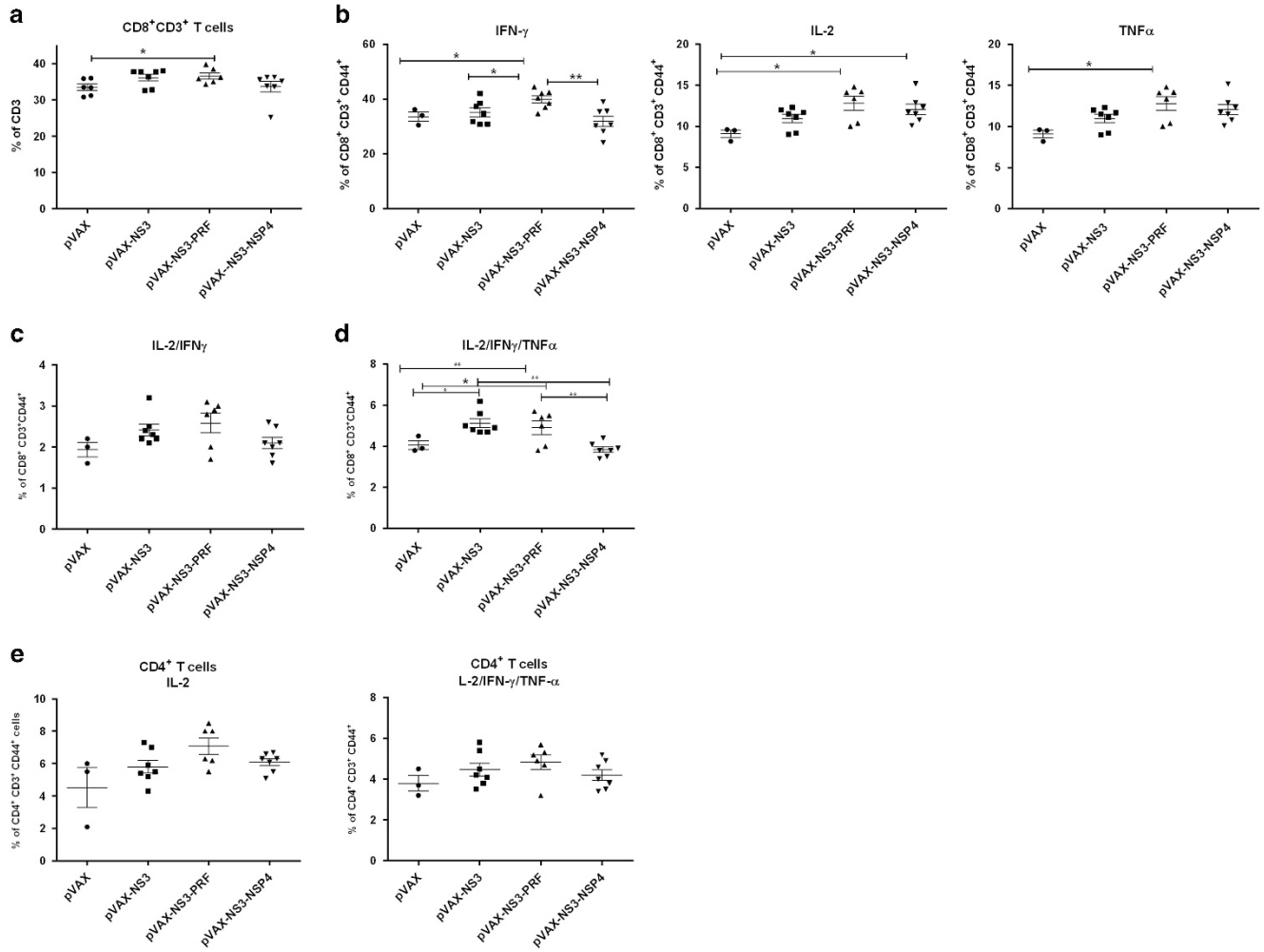

Figure 5. Cytokine profile of the NS3-specific $CD4^+$ and $CD8^+$ T cells in vaccinated mice. Splenocytes from mice vaccinated with pVAX, pVAX-NS3, pVAX-NS3-PRF or pVAX-NS3-NSP4 were harvested 10 days after vaccination. Intracellular cytokine staining was performed and the cells were gated on CD3, CD44 and then CD4 or CD8 to assess the frequency of (**a**) $CD3^+$ $CD8^+$ T cells, (**b**) $CD8^+$ $CD44^+$ effector memory T cells that are single cytokine producers of IFN-γ or IL-2 or TNF-α, (**c**) $CD8^+$ $CD44^+$ effector memory T cells that are double cytokine producers of IL-2/IFN-γ, (**d**) IFN-γ/TNF-α/IL-2 triple-positive $CD8^+$ $CD44^+$ effector memory T cells and (**e**) IL-2- producing $CD4^+$ $CD44^+$ T cells and IFN-γ/TNF-α/IL-2 triple-positive $CD4^+$ $CD44^+$ T cells. Each symbol represents an individual mouse and data show mean ± s.e.m. $^*P < 0.05$ and $^{**}P < 0.01$.

of NS3 with the effect of the adjuvant activity of PRF. The results of this experiment showed that coexpression NS3 and NSP4 resulted in a significantly attenuated immune response to NS3 when compared with pVAX-NS3-PRF-vaccinated mice for pools 2, 3 and intradermally (Figure 4). In fact, the number of spot-forming units observed in mice vaccinated with pVAX-NS3-NSP4 was comparable, but lower compared with those observed in pVAX-NS3 mice, especially for pool 3 ($P < 0.05$) and pool 2 (NS).

Intracellular cytokine staining demonstrated that only the mice that were vaccinated with pVAX-NS3-PRF showed a significantly higher frequency of NS3-specific CD8 T cells (Figure 5a). These mice also had a greater frequency of CD8 effector memory T cells secreting IFN-γ, when compared with pVAX-, pVAX-NS3- or pVAX-NS3-NSP4-vaccinated mice (Figure 5b). Only mice vaccinated with pVAX-NS3-PRF or pVAX-NS3-NSP4 had a greater frequency of interleukin-2 (IL-2)-secreting CD8 effector memory T cells, whereas only vaccination with pVAX-NS3-PRF induced a greater frequency of tumour necrosis factor-α (TNF-α)-secreting CD8 effector memory T cells (Figure 5b). Both pVAX-NS3- and pVAX-NS3-PRF-vaccinated mice showed a trend toward an increase in double cytokine producers of IL-2 and IFN-γ (Figure 5c).

Mice vaccinated with pVAX-NS3 or pVAX-NS3-PRF showed a significant increase in rare, multifunctional CD8 T cells that secreted TNF-α, IFNγ and IL-2 simultaneously when compared with pVAX- or pVAX-NSP4-vaccinated mice (Figure 5d). There was no difference in triple cytokine producers between pVAX-NS3 and pVAX-NS3-PRF. Although there was a trend toward an increase in CD4 effector memory T cells secreting IL-2 and multifunctional triple cytokine producers (Figure 5e), it was not significant.

Collectively, these results show that the inclusion of PRF significantly increased the overall NS3-specific CMI in vaccinated mice, including responses to $CD8^+$-restricted epitopes. Importantly, the results indicate that the inclusion of a recognised apoptotic gene, *NSP4*, resulted in a detrimental effect on the immunogenicity of NS3 and emphasised the divergent mode of action of PRF, the expression of which increased NS3 immunogenicity.

Vaccinated mice show $CD8^+$ T-cell-dependent protection in an HCV surrogate hepatic challenge model

To determine if the enhanced NS3-specific CMI generated after vaccination with pVAX-NS3-PRF resulted in increased protection,

© 2016 Macmillan Publishers Limited

vaccinated mice were challenged with our recently described *in vivo* hepatic challenge model.[49] In this model, HCV proteins are expressed in the hepatocytes of immunocompetent mice after hydrodynamic injection of a plasmid (termed pNFS) encoding the wild-type HCV NS3/4A protein and secreted alkaline phosphatase (SEAP), which is measured in the serum as a surrogate marker for the intrahepatic expression of the NS3/4A protein. This model permits longitudinal analysis of the clearance of HCV antigen-positive hepatocytes in previously vaccinated mice, as the levels of secreted SEAP in the sera of vaccinated animals directly correlate with antigen expression in the liver.[49] Three groups of mice were vaccinated, and 10 days after the final dose, they were challenged by hydrodynamic injection of the NS3/4A plasmid (pNFS). The SEAP levels were measured on days 4, 7 and 11 after challenge.

The results showed that the SEAP levels in the pVAX-NS3- and pVAX-NS3-PRF-vaccinated groups were reduced at each time point compared with the control group. On day 4, the difference in the level of SEAP in serum between the control group and the pVAX-NS3 group was significant ($P < 0.05$), whereas the difference between that in the control group and the pVAX-NS3-PRF group was highly significant ($P < 0.01$). On days 7 and 11, the difference was highly significant in the pVAX-NS3 and pVAX-NS3-PRF groups compared with the control group ($P < 0.01$; Figure 6a). Although the mouse challenge model failed to show a statistically significant difference in protection between the NS3 group and NS3-PRF groups, the mean value of SEAP in the NS3-vaccinated group was higher compared with that in the NS3-PRF-vaccinated group, which is most likely because the latter group has greater CMI to NS3, which could facilitate more efficient clearance of hepatocytes that express NS3. This difference in vaccine efficacy could be important to protect more effectively against a spreading infection with HCV, as opposed to the static expression of HCV NS3 antigen in this model.

To confirm that protection was provided by NS3-specific $CD8^+$ T cells, we vaccinated three groups of mice (pVAX, pVAX-NS3 and pVAX-NS3-PRF) and divided each group into two subgroups. The $CD8^+$ T cells in one subgroup from each vaccinated group were depleted by intraperitoneal injection of 0.1 mg of anti-CD8 antibodies (Figure 6b) and the SEAP level was measured on days 1 and 7 after challenge in all animals. Day 7 values were normalised to the respective day 1 values to calculate a percentage SEAP level. When the 50% maximum (dashed line in Figure 6b) SEAP level fold change was plotted for each group, all the CD8-undepleted mice from the pVAX-NS3- and pVAX-NS3-PRF-vaccinated groups were below the 50% cutoff. In contrast, in the respective CD8-depleted subgroups of pVAX-NS3- and pVAX-NS3-PRF-vaccinated mice, 9/10 mice were above the cutoff. As expected, there were no differences in the SEAP levels between the depleted and undepleted subgroups in the pVAX control group (Figure 6c).

Furthermore, the results showed that the SEAP levels in the vaccinated groups, which were $CD8^+$ T-cell-depleted, were similar to that in the unvaccinated group, confirming that the reduction in SEAP level in the serum (and thus HCV NS3-positive hepatocytes) was $CD8^+$ T-cell-dependent (Figure 6c).

The inclusion of PRF in DNA vaccines increased NS3-specific CMI in pigs

Vaccines that are effective in mice should be evaluated for efficacy in a large animal model before human studies. Pigs are recognised as the closest animal model to humans, next to primates; hence, they serve as an ideal preclinical model to test the translational potential of our vaccines.[33] Outbred White Landrace pigs were immunised intradermally with 300 µg of either pVAX-NS3 or pVAX-NS3-PRF using a microneedle device to ensure reproducible

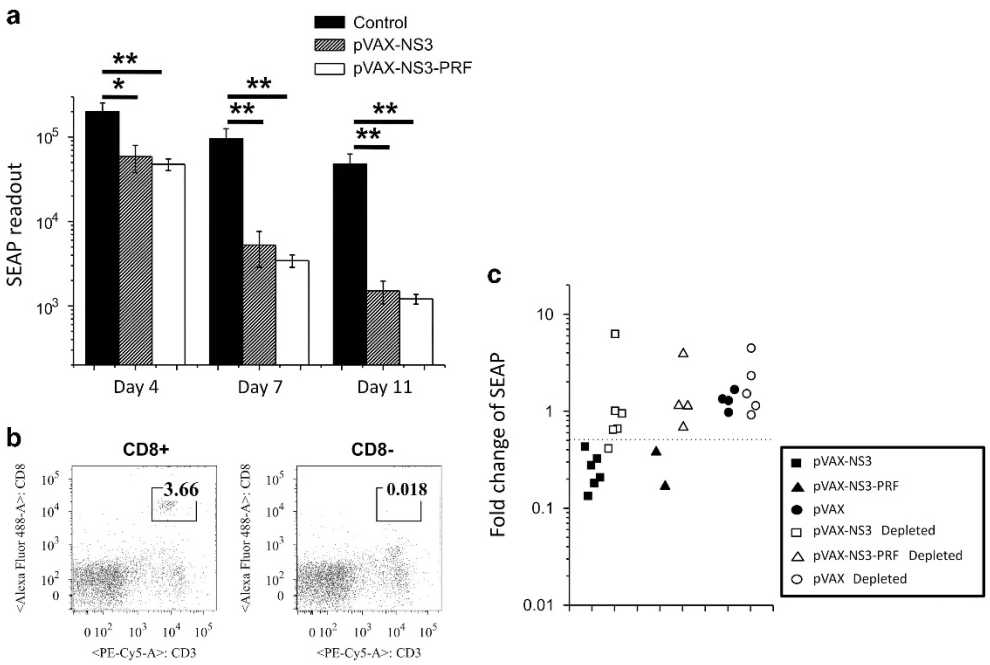

Figure 6. Vaccination with pVAX-NS3-PRF results in increased protection against challenge. (**a**) Groups of mice vaccinated with pVAX only ($n = 10$), pVAX-NS3 ($n = 12$) or pVAX-NS3-PRF ($n = 12$) were challenged with 20 µg pNFS by hydrodynamic injection. SEAP was measured on days 4, 7 and 11 after challenge in the serum of individual mice. (**a**) Groups of mice were vaccinated and challenged as described in panel a. The mice from each group were split into two subgroups, which were designated as +/− $CD8^+$ T-cell-depleted (pVAX $n = 9$, 5 with depletion; pVAX-NS3 $n = 12$, 6 with depletion; or pVAX-NS3-PRF $n = 6$, 4 with depletion). (**b**) $CD8^+$ T-cell depletion was performed 3 h after the challenge and depletion was confirmed by flow cytometry. Representative dot plots from each group (CD8+ or CD8− mice) are presented. (**c**) The SEAP level was then measured in all mice on days 1 and 7. All day 7 values were normalised to the respective day 1 values to calculate a fold change in the SEAP level. *$P < 0.05$, **$P < 0.01$.

© 2016 Macmillan Publishers Limited

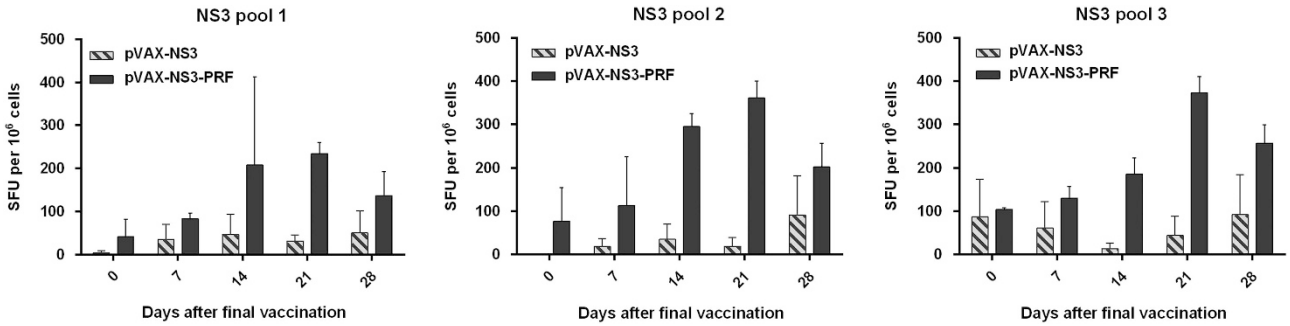

Figure 7. Immunisation with a DNA vaccine encoding HCV NS3 and PRF elicits strong NS3-specific CMI in pigs. Two groups of 6-week-old outbred White Landrace pigs were immunised intradermally three times with 300 μg of DNA (pVAX-NS3 or pVAX-NS3-PRF) at 2-week intervals. PBMCs were collected and HCV NS3-specific T-cell responses were measured by IFN-γ production in ELISpot after peptide stimulation as described in the methods above. Data represent mean spot-forming units (SFU) per 10^6 splenocytes (± s.e.m).

delivery of the vaccine. Each pig received three doses of the vaccine at 2-week intervals and peripheral blood mononuclear cells (PBMCs) were isolated on different days for subsequent analysis by IFN-γ ELISpot. The results show that there was a clear increase in the NS3-specific IFN-γ response in the pVAX-NS3-PRF-vaccinated pigs compared with the pVAX-NS3-vaccinated pigs (Figure 7). As the pig numbers are small, it was not possible to perform statistical analysis. However, the responses in the pVAX-NS3-PRF-vaccinated animals were higher at all time points, particularly 3 weeks after final boost across all NS3 peptide pools. Thus, coexpression of NS3 and PRF after vaccination with the DNA vaccine appeared to have an adjuvant effect and enhanced the CMI to NS3 in pigs.

DISCUSSION

In this study, we have further defined the use of PRF as a cytolytic adjuvant to increase the efficacy of a DNA vaccine for HCV. The results of this study show that PRF induced cell death in vaccine-targeted cells, increased the level of NS3-specific responses in mice, increased the protection mediated by $CD8^+$ T cells in a surrogate challenge model and increased the CMI to NS3 in a large animal model, viz. the pig.

As unambiguous identification of the mechanism of cell death is difficult,[50,51] we showed that the expression of PRF-positive cells resulted in non-apoptotic cell death, which most likely occurs by necrosis that is mediated through the RIP1 kinase pathway.

Normally PRF is expressed primarily by natural killer cells and cytotoxic T lymphocytes. Taken together with granzymes released by the same cell, PRF functions in a Ca^{2+}-dependent pathway during NK- and CTL-induced cytolysis of target cells by creating pores in the plasma membrane (reviewed by Voskoboinik *et al*.[52]). Unlike granzymes, the toxicity of PRF is less well characterised, but its activity is highly dependent on pH and Ca^{2+}. Previously, it has been reported that the C-terminal truncated PRF (PRF-12), as used in this study, fails to be exported from the endoplasmic reticulum and is highly toxic to the host cell.[34,53] It is proposed that the concentration of Ca^{2+} in the endoplasmic reticulum activates PRF to form pores and as a consequence activates cell death pathways involved in regulated necrosis in PRF-transfected cells (reviewed in Voskoboinik *et al*.[52]).

Furthermore, in response to a given death stimulus, even to a specific dose of a cytotoxic agent, a continuum of apoptosis and necrosis coexists in the same cell. Many agents induce apoptosis at low doses and necrosis at higher doses, and we believe this to be the case in pVAX-NS3-PRF-transfected cells. Our data and other studies support the notion that overexpression of intracellular NS3 triggers apoptotic cell death. Others have shown that HCV NS3 binds to caspase-8 through its DEVD and alters the cellular distribution of the caspase.[41] However, PRF-induced necrosis is more effective and alters the NS3/PRF balance towards necrosis, resulting in enhanced immunogenicity of NS3. Elucidating the exact mechanism of PRF-mediated necrosis will be the focus of further studies.

The promise of DNA vaccines in mice has not been reproduced in humans, although the problem is unrelated to body mass.[54] We believe that the cytolytic gene technology represents an effective mechanism to target APCs, including DCs, indirectly. DCs are the major APCs that are able to prime naive T cells, and although direct presentation of epitopes results from endogenous expression of the immunogen in DCs, cross-presentation is a more common pathway to induce immunity to viruses (or vaccines), which do not directly infect or target DCs.[17] Our previous work has shown that vaccination with the PRF-encoding vaccine resulted in an increased frequency of activated $CD11c^+$ $CD8a^+$ DCs in the lymph nodes draining the site of immunisation, a cell population that is essential for cross-presentation of antigens from dying cells to naive CD8 T cells.[18] There is a necessity for a threshold level of antigen expression, which is necessary for robust immune responses in our system. Our previous data suggest that the timing of cell death and the level of antigen expression are linked.[18] The uptake of viral antigen-positive dead or dying cells by DCs and other APCs represents a fundamental mechanism to elicit immunity against pathogens that do not intrinsically infect DCs and we have exploited this natural mechanism to enhance vaccine efficacy. We show that the T-cell-mediated immune responses following vaccination were significantly enhanced by the coexpression of PRF, as determined by increased responses to all NS3 peptides in ELISpot and increased numbers of effector memory CD8 T cells that secreted IFNγ, IL-2 and TNF-α in response to stimulation by NS3 peptides. The addition of PRF also broadened the immune response by enhancing T-cell responses to nondominant epitopes.

Conversely, proapoptotic NSP4 failed to enhance immune responses, but instead reduced the strength of the immune response to some NS3 epitopes. This is not surprising as NSP4 disrupts mitochondrial membrane potential, eliciting an intrinsic apoptotic pathway,[26] and as NS3 is also proapoptotic, antigen-positive cells become completely apoptotic and are cleared in a non-inflammatory manner before they can undergo secondary necrosis,[23] thus limiting the activation of DC and subsequent cross-presentation of NS3.

Importantly, the adjuvant activity of PRF was also evident in the enhanced NS3 responses observed in the preclinical, large animal model. As shown in the pig vaccination studies, the strategy increased the magnitude of the initial effector cell response, and as this dictates the magnitude of the population of central memory T cells, measures taken to optimise this response will

© 2016 Macmillan Publishers Limited

increase the overall vaccine efficacy.[54] Thus, a cytolytic/necrotic DNA vaccine might not only result in increased efficacy in a DNA prime/virus vector boost regimen but may also elicit effective CMI in a multidose homologous regimen, providing the advantages of a simple DNA vaccine, including the lack of induced immunity to the vector.

Innate immune responses are activated by pathogen-associated molecular patterns (PAMPs) (including viral antigens and nucleic acids) or damage-associated molecular patterns, as a prelude to adaptive immune responses. We and others have previously encoded natural adjuvants or cytokines in a DNA vaccine,[20,55,56] but we believe that our DNA vaccine, which induces necrotic death in vaccine-targeted cells, would be more effective because it is more likely to activate a wider range of transcriptional pathways, leading to more effective immunity. Our previous study demonstrated that using PRF to induce death of viral antigen-positive cells resulted in increased protection against challenge with a chimeric HIV, EcoHIV, in which the gp120 envelope protein was replaced with gp80 from mouse leukaemia virus.[18] In this study, we applied this strategy to an HCV DNA vaccine and showed that it increased NS3-specific CMI in mice and pigs. The slight increase in protective immunity detected after 'challenge' with the hydrodynamic DNA differs to that after challenge with EcoHIV in mice vaccinated with a DNA vaccine that encoded gag and PRF, as the gag/PRF vaccine elicited a statistically significant reduction in the viral load.[18] The lack of significance after vaccination with the NS3/PRF vaccine may reflect differences in the challenge model as the levels of NS3 antigen expressed in the liver after hydrodynamic injection are likely to be considerably higher compared with the levels of HIV protein produced after infection with EcoHIV. Nevertheless, the fact that the NS3-PRF vaccine was more effective at early time points after pNFS 'challenge' may be vital in the race between the anamnestic response and HCV replication in previously vaccinated, challenged individuals.

The skin is the first line of defence against invading pathogens and contains specialised immune cells, especially professional APCs such as DCs. We have exploited this characteristic to deliver our DNA vaccine, but the practice of intradermal injection may result in considerable variation after conventional needle/syringe delivery. We have overcome this issue in the pig by using the microneedle device, which deposits the payload into the shallow layers of the skin in a highly consistent manner. These studies and other preclinical studies ongoing in our laboratory suggest that a DNA vaccine encoding a suitable immunogen and PRF is a candidate for human clinical trials.

MATERIALS AND METHODS

DNA vaccines

A codon-optimised HCV NS3 genotype 1b gene was synthesised (Gene Art, Regensburg, Germany) and inserted into pVAX (Thermo Fisher Scientific Inc.) downstream of the CMV promoter. A second promoter, the SV40 promoter, and a polyadenylation signal were also inserted into pVAX, and a C-terminal-truncated mouse PRF (*PRF-12*) gene[57] or the rotavirus NSP4[58] were inserted downstream of this promoter. As a control in the LDH and caspase-3 activity assays, the truncated *PRF* gene was inserted downstream of the CMV promoter in another construct (pCMV-PRF). All DNA plasmids were sequenced to ensure correct nucleotide sequence and the vaccines were purified using an Endotoxin-Free Mega Kit (Qiagen, VIC, Australia).

Cell culture

HEK293T and Huh-7 cells were cultured at 37 °C in 5% CO_2 in Dulbecco's modified Eagle's medium (DMEM) supplemented with 10% foetal calf serum and 1% penicillin/streptomycin. Six hours after the transfection, media containing Lipofectamine LTX (Life Technologies, Scoresby, VIC, Australia) and DNA were replaced with reduced serum (2%) DMEM for the duration of experiments.

Western blot analysis

To detect NS3 expression, HEK293T cells were transiently transfected with 2.5 μg of pVAX-NS3 or pVAX-NS3-PRF DNA in six-well plates using Lipofectamine LTX following the manufacturer's recommendations. The cells were incubated for 48 h, the cell lysates harvested and the concentration of proteins determined using the Pierce BCA Protein Assay Kit (Thermo Fisher Scientific Inc.). A polyclonal anti-NS3 antibody (g1b; Virostat, Westbrook, ME, USA) was used to detect NS3 expression. The membrane was developed by extreme sensitivity chemiluminescence substrate (Western Lightning Ultra; Perkin-Elmer, Glen Waverly, VIC, Australia) and imaged by LAS 4000 digital imaging system (Fujifilm, Keswick, SA, Australia). For the expression of cytokeratin 18, Huh-7 cells were seeded overnight in six-well plates and transfected with 2.5 μg DNA per well. Additional cells were treated with 1 or 2 μM doxorubicin, the foetal bovine serum concentration reduced to 5% and the cells then analysed by western blot. The primary antibody was rabbit anti-CK18 (Santa Cruz Biotechnology, Dallas, TX, USA) at a dilution of 1:7000, whereas the secondary antibody was horse radish peroxidase-conjugated goat anti-rabbit IgG (Antibodies Australia, Monash University, VIC, Australia) at 1:10 000. The membrane was developed as described above.

Immunofluorescence

To detect the expression of PRF and NS, HEK293T cells were transiently transfected with 200 ng of pVAX, pVAX-NS3 or pVAX-NS3-PRF in 96-well plates. Two days after transfection, the cells were fixed with 4% formalin (Sigma, Castle Hill, NSW, Australia) for 20 min, permeabilised with methanol at − 20 °C and then blocked in 2.5% bovine serum albumin (Sigma) in phosphate-buffered saline. Primary antibodies, mouse anti-HCV gt1b (Virostat) and rat anti-PRF (Abcam, Melbourne, VIC, Australia), were diluted in 1% bovine serum albumin (Sigma), 0.3% Triton X-100 (Sigma) in phosphate-buffered saline and incubated overnight at 4 °C. After washing, the cells were then incubated for 1 h with fluorophore-conjugated secondary antibodies (1:300) viz. anti-mouse-FITC (eBioscience, San Diego, CA, USA) or goat anti-rat-Cy5 (Life Technologies). Cells were visualised by fluorescent microscopy (Zeiss LSM-700, Carl Zeiss Pty Ltd, North Ryde, NSW, Australia).

LDH release assay

The LDH assay was performed by using the Pierce LDH Cytotoxicity Assay Kit (Thermo Fisher Scientific Inc.) following the manufacturers' protocol. In brief, 2×10^4 HEK293T cells were seeded in 10% foetal calf serum/DMEM in 96-well plates and transfected with 200 ng of plasmid DNA in triplicate in the presence or absence of 10 μM necrostatin-1 (Sigma-Aldrich, Castle Hill, NSW, Australia) or PAN caspase inhibitor zVAD-FMK (Calbiochem, Merck Millipore, Bayswater, VIC, Australia). Eight hours after transfection, the media were replaced with low serum (2%) DMEM. Cell culture supernatants were sampled at 48 h after transfection. Cytotoxicity was calculated as a percentage of maximum specific lysis. Apoptotic control cells were induced by the addition of 2 μM doxorubicin. To measure cell death, cell culture supernatants were sampled in triplicate at 24 and 48 h after transfection and readings were presented as a percentage normalised to the maximum LDH activity.

Measurement of DEVD-caspase activity

DEVD-caspase activity was assayed by cleavage of zDEVD-AFC, a fluorogenic substrate based on the peptide sequence at the caspase-3 cleavage site of poly(ADP) ribose polymerase, as described previously.[59] Briefly, HEK293T cells (2×10^4) were cultured 10% fetal calf serum/DMEM in 96-well plates, transfected with 200 ng of plasmid DNA (in triplicate) in the presence or absence of PAN caspase inhibitor (zVAD-FMK). Eight hours after transfection, the medium was replaced with low serum medium (2% fetal calf serum/DMEM). At 48 h after transfection, cells were scraped and pelleted, washed once with phosphate-buffered saline and resuspended in 200 μl NP-40 lysis buffer (containing 5 mmol l^{-1} Tris-HCl, 5 mmol l^{-1} EDTA and 0.5% NP-40 (pH7.5)). The protein content of cell lysates was quantified using the standard Bradford protein assay and 20 μg of each sample was used in the caspase activity assay. Cell lysates were added to fluorometric buffer (containing 8 μmol l^{-1} substrate in 1 ml protease buffer (50 mmol l^{-1} HEPES, 10% sucrose, 10 mmol l^{-1} dithiothreitol, 0.1% CHAPS (pH7.4)). After incubation in the dark for 4 h at room temperature, fluorescence was quantified (excitation 400 and emission 500) in the Optima Fluostar (BMG Labtech, Mornington, VIC, Australia).

© 2016 Macmillan Publishers Limited

Flow cytometry

Huh-7 cells were transfected with 2.5 μg of pVAX-NS3 or pVAX-NS3-PRF, and 48 h after transfection they were stained by Annexin V-FITC (Life Technologies) and PI (BD Pharmingen, North Ryde, NSW, Australia) in 100 μl Annexin V binding buffer at room temperature for 15 min. Annexin V binding and PI uptake were measured by flow cytometry using a Becton Dickinson FACS Canto flow cytometer (Becton Dickinson, San Jose, CA, USA).

Splenocytes were harvested from vaccinated mice 10 days after vaccination and multicolour intracellular cytokine staining was performed on splenocytes stimulated with 4 μg ml^{-1} HCV peptides representing immunodominant NS3 CD8 T-cell epitopes for 12 h in the presence of protein transport inhibitor (BD GolgiStop, BD Biosciences, North Ryde, NSW, Australia). Staining was performed with BD FACS Cytofix/Cytoperm and BD anti-mouse antibodies: CD3-PerCP-Cy5.5, CD8-APC-Cy7, CD44-APC, IL-2-FITC, IFN-γ-PE-Cy7 and TNF-α-PE (BD Biosciences). The cells were analysed on a Becton Dickinson FACS Canto II flow cytometer using the gating strategy described previously.[18,20] Briefly, splenocytes were gated on the lymphocyte population, followed by doublet discrimination and then gated on CD3$^+$ and CD44$^+$ cells, and finally CD4$^+$ or CD8$^+$ cell to assess the frequency of IFN-γ-, TNF-α- and IL-2-secreting cells. The results were analysed with the FlowJo X.0.7 software (FlowJo, Ashland, OR, USA).

Animals

Female C57BL/6 mice aged 6–8 weeks were obtained from The University of Adelaide, Animal Laboratory Services. Mice for the ELISpot study were housed in the Women's and Children's Hospital animal house. Mice for the challenge experiment were housed in the Queen Elizabeth Hospital animal house. All experimental protocols were approved by the Animal Ethics Committee of the Women's and Children's Health Network, the University of Adelaide and South Australia Pathology. White Landrace pigs were obtained from the University of Adelaide Roseworthy Campus and were housed at the Large Animal Research Facility, South Australian Health and Medical Research Institute. All experimental protocols in pigs were approved by the University of Adelaide and the South Australia Pathology Animal Ethics Committees.

Immunisations

C57BL/6 mice were immunised intradermally with 50 μg of pVAX, pVAX-NS3, pVAX-NS3-PRF or pVAX-NS3-NSP4 DNA (50 μg in 50 μl saline) injected into the dermal layer of the ear as described previously.[18,55,60] The mice received a total of three doses at 2-week intervals. At 10 days after vaccination, the mice were killed and splenocytes were prepared for the analysis.

In the pig trial, 6-week-old outbred White Landrace pigs were randomly allocated to two groups of two, and each was immunised intradermally with either 300 μg of pVAX-NS3 or pVAX-NS3-PRF DNA (in saline). To ensure reproducible delivery of DNA, the immunisations were performed using a microneedle device (FluGen Inc., Madison, WI, USA), which delivered the DNA in a volume of 250 μl of saline. Each pig received three doses of the DNA vaccine at 2-week intervals in the upper inner front leg. The pigs were bled aseptically through the jugular vein and PBMCs were purified for analysis.

Peptides used for stimulation

A panel of 98 overlapping 15–19 mer peptides spanning the entire NS3 protein (strain J4L6S, genotype 1b) was obtained from the National Institutes for Health Bio Defense and Emerging Infectious Research Resources Repository, NIAID, National Institutes of Health (Bethesda, MD, USA). Individual peptides overlap by 11–12 amino acids and detailed information on their length and sequence is provided by BEI Resourses (http://www.beiresources.org/Catalog/BEIPeptideArrays/NR-3742.aspx).
The peptides were divided into three pools, each containing 29–31 individual peptides. Two epitopes, restricted to C57BL6 (H-2^b) CD8+ T cells, were described previously,[48] and were used as the CD8 immunodominant pool to stimulate splenocytes in ELISpot and intracellular cytokine staining. All peptides were used at a final concentration of 4 μg ml^{-1}.

IFNγ ELISpot

Mouse IFNγ ELISpot was performed on red blood cell-depleted splenocytes that were restimulated for 36 h at 37 °C with the peptide pools. To assay IFNγ production by restimulated porcine PBMCs, cryopreserved cells were thawed and treated with 50 U of benzonase (Sigma-Aldrich) at 37 °C for 10 min. The PBMCs were then washed and resuspended in culture media and restimulated with the NS3 peptide pools for 20 h at 37 °C.

Multiscreen-IP HTS plates (Millipore, Bayswater, NSW, Australia) were coated with anti-mouse IFNγ (clone AN18; MabTech, Stockholm, Sweden) for mouse ELISpot or with anti-porcine IFNγ (MabTech) for porcine ELISpot. Secreted IFNγ was detected with anti-mouse IFNγ-biotin (clone R4-6A2; MabTech) or anti-pan IFNγ-biotin (MabTech), followed by streptavidin-AP (Sigma) and SigmaFast BCIP/NBT (Sigma-Aldrich). Phytohaemagglutinin-stimulated cells (5 μg ml^{-1}) were used as a positive control and unstimulated splenocytes or porcine PBMCs cultured in the media represented the negative controls. Developed spots were counted automatically using an ELISpot reader (AID GmbH, Strasburg, Germany).

Mouse challenge

Three groups of mice were immunised as described above. At 10 days after vaccination, the mice were injected with 20 μg pNFS plasmid in TransIT-QR HD delivery solution (Mirus, Madison, WI, USA) in a volume of 1/10th body weight as we described previously.[49] In the pNFS plasmid, NS3/4A protein expression is controlled by the mouse albumin promoter/α-fetoprotein enhancer ensuring hepatocyte-specific expression. Introns 1 and 2 were included to optimise the expression. SEAP expression is encoded as a fusion protein, preceded by the FMDV2A protease, which is designed to self-cleave and release SEAP cotranslationally.

Any mouse that failed to receive the full volume was excluded from further analysis. Challenged mice were bled at different time points and SEAP activity in the serum was detected using the Phospha-Light Kit (Applied Biosystems, Scoresby, VIC, Australia) in 96-well flat-bottom white microplates (Greiner BioOne, WestHeidelberg, VIC, Australia). Details of pNFS and the SEAP assay were described elsewhere.[49] CD8$^+$ cells were depleted in mice that were successfully challenged with pNFS and rested for 4 h following the challenge. For CD8$^+$ cell depletion, a single dose of 0.1 mg of purified endotoxin-free anti-CD8a (clone 53-6.7; eBioscience) was delivered via the intraperitoneal route.

Statistical analysis

Throughout the study, statistical analysis was performed by Kruskal–Wallis multiple comparison with Wilcoxon's post-tests, to allow for nonparametric data and to correct for multiple comparisons. Data in graphs are presented as the mean ± s.e.m. Data analysis and generation of graphs were performed using GraphPad Prism 5.0b (Graph Pad Software Inc, La Jolla, CA, USA) and SAS Version 9.3 (SAS, Lane Cove, NSW, Australia) with assistance from Dr Start Howell from the Data Analysis and Management Centre, University of Adelaide. Nonparametric Kruskal–Wallis test was used to compare the difference between the multiple vaccine groups. If the global test showed significant difference between the groups, then Wilcoxon's tests were performed to compare the *post hoc* difference between groups.

Ethics statement

The mouse experiments were reviewed and approved by the Women's and Childrens' Hospital, the University of Adelaide and the SA Pathology animal ethics committees as project numbers AE783/02/2012, M-2012-210 and 19a/13, respectively, whereas the pig experiments were reviewed and approved as project numbers M-2012-177 R and 14b/13, respectively. The protocols adhered to the Australian code for the care and use of animals for scientific purposes 8th edition (2013), published by the National Health and Medical Research Council (NHMRC).

CONFLICT OF INTEREST

The authors declare no conflict of interest.

ACKNOWLEDGEMENTS

We thank Dr Paul Radspinner (FluGen Inc., Madison, WI, USA) who provided the microneedle device and Renee Herber for training to use the device. We also thank Dr John Taylor (University of Auckland, New Zealand) and Dr Barbara Coulson (University of Melbourne, Australia) for the gift of the NSP4 construct. We acknowledge the kind gift of the HCV peptide pools, which were obtained through the AIDS Reagent and Reference Reagent Program, Division of AIDS, NIAID, National Institutes of Health, USA. We also thank Dr Stuart Howell for statistical advice.

© 2016 Macmillan Publishers Limited

This research was supported by grants APP1026293, 543139 and 543143 from the National Health and Medical Research Council (NHMRC) of Australia, grant BF040005 from the Australian-Indian biotechnology fund and a grant from the Hospital Research Foundation (THRF). DW is a Research Fellow supported by THRF.

REFERENCES

1 World Health Organization. *Hepatitis C, Fact Sheet No.164*. World Health Orgnization: Geneva, Switzerland, 2014.
2 Reau NS, Jensen DM. Sticker shock and the price of new therapies for hepatitis C: is it worth it? *Hepatology* 2014; **59**: 1246–1249.
3 Liang TJ. Current progress in development of hepatitis C virus vaccines. *Nat Med* 2013; **19**: 869–878.
4 Torresi J, Johnson D, Wedemeyer H. Progress in the development of preventive and therapeutic vaccines for hepatitis C virus. *J Hepatol* 2011; **54**: 1273–1285.
5 Micallef JM, Kaldor JM, Dore GJ. Spontaneous viral clearance following acute hepatitis C infection: a systematic review of longitudinal studies. *J Viral Hepat* 2006; **13**: 34–41.
6 Thimme R, Oldach D, Chang KM, Steiger C, Ray SC, Chisari FV. Determinants of viral clearance and persistence during acute hepatitis C virus infection. *J Exp Med* 2001; **194**: 1395–1406.
7 Frick DN. The hepatitis C virus NS3 protein: a model RNA helicase and potential drug target. *Curr Issues Mol Biol* 2007; **9**: 1–20.
8 Takaki A, Wiese M, Maertens G, Depla E, Seifert U, Liebetrau A *et al.* Cellular immune responses persist and humoral responses decrease two decades after recovery from a single-source outbreak of hepatitis C. *Nat Med* 2000; **6**: 578–582.
9 Major ME, Mihalik K, Puig M, Rehermann B, Nascimbeni M, Rice CM *et al.* Previously infected and recovered chimpanzees exhibit rapid responses that control hepatitis C virus replication upon rechallenge. *J Virol* 2002; **76**: 6586–6595.
10 Nascimbeni M, Mizukoshi E, Bosmann M, Major ME, Mihalik K, Rice CM *et al.* Kinetics of CD4+ and CD8+ memory T-cell responses during hepatitis C virus rechallenge of previously recovered chimpanzees. *J Virol* 2003; **77**: 4781–4793.
11 Gerlach JT, Ulsenheimer A, Gruner NH, Jung MC, Schraut W, Schirren CA *et al.* Minimal T-cell-stimulatory sequences and spectrum of HLA restriction of immunodominant CD4+ T-cell epitopes within hepatitis C virus NS3 and NS4 proteins. *J Virol* 2005; **79**: 12425–12433.
12 Ulsenheimer A, Lucas M, Seth NP, Tilman Gerlach J, Gruener NH, Loughry A *et al.* Transient immunological control during acute hepatitis C virus infection: ex vivo analysis of helper T-cell responses. *J Viral Hepat* 2006; **13**: 708–714.
13 Li L, Saade F, Petrovsky N. The future of human DNA vaccines. *J Biotechnol* 2012; **162**: 171–182.
14 Cai Y, Rodriguez S, Hebel H. DNA vaccine manufacture: scale and quality. *Expert Rev Vaccines* 2009; **8**: 1277–1291.
15 Romani N, Flacher V, Tripp CH, Sparber F, Ebner S, Stoitzner P. Targeting skin dendritic cells to improve intradermal vaccination. *Curr Top Microbiol Immunol* 2012; **351**: 113–138.
16 Pasparakis M, Haase I, Nestle FO. Mechanisms regulating skin immunity and inflammation. *Nat Rev Immunol* 2014; **14**: 289–301.
17 Heath WR, Belz GT, Behrens GM, Smith CM, Forehan SP, Parish IA *et al.* Cross-presentation, dendritic cell subsets, and the generation of immunity to cellular antigens. *Immunol Rev* 2004; **199**: 9–26.
18 Gargett T, Grubor-Bauk B, Garrod TJ, Yu W, Miller D, Major L *et al.* Induction of antigen-positive cell death by the expression of perforin, but not DTa, from a DNA vaccine enhances the immune response. *Immunol Cell Biol* 2014; **92**: 359–367.
19 Gargett T, Grubor-Bauk B, Miller D, Garrod T, Yu S, Wesselingh S *et al.* Increase in DNA vaccine efficacy by virosome delivery and co-expression of a cytolytic protein. *Clin Transl Immunol* 2014; **3**: e18.
20 Gummow J, Li Y, Yu W, Garrod T, Wijesundara D, Brennan AJ *et al.* A multi-antigenic DNA vaccine that induces broad HCV-specific T-cell responses in mice. *J Virol* 2015; **89**: 7991–8002.
21 Lowin B, Hahne M, Mattmann C, Tschopp J. Cytolytic T-cell cytotoxicity is mediated through perforin and Fas lytic pathways. *Nature* 1994; **370**: 650–652.
22 Law RH, Lukoyanova N, Voskoboinik I, Caradoc-Davies TT, Baran K, Dunstone MA *et al.* The structural basis for membrane binding and pore formation by lymphocyte perforin. *Nature* 2010; **468**: 447–451.
23 Rock KL, Lai JJ, Kono H. Innate and adaptive immune responses to cell death. *Immunol Rev* 2011; **243**: 191–205.
24 Sancho D, Joffre OP, Keller AM, Rogers NC, Martinez D, Hernanz-Falcon P *et al.* Identification of a dendritic cell receptor that couples sensing of necrosis to immunity. *Nature* 2009; **458**: 899–903.
25 Zelenay S, Keller AM, Whitney PG, Schraml BU, Deddouche S, Rogers NC *et al.* The dendritic cell receptor DNGR-1 controls endocytic handling of necrotic cell antigens to favor cross-priming of CTLs in virus-infected mice. *J Clin Invest* 2012; **122**: 1615–1627.
26 Bhowmick R, Halder UC, Chattopadhyay S, Chanda S, Nandi S, Bagchi P *et al.* Rotaviral enterotoxin nonstructural protein 4 targets mitochondria for activation of apoptosis during infection. *J Biol Chem* 2012; **287**: 35004–35020.
27 Ball JM, Mitchell DM, Gibbons TF, Parr RD. Rotavirus NSP4: a multifunctional viral enterotoxin. *Viral Immunol* 2005; **18**: 27–40.
28 Ahlen G, Soderholm J, Tjelle T, Kjeken R, Frelin L, Hoglund U *et al. In vivo* electroporation enhances the immunogenicity of hepatitis C virus nonstructural 3/4A DNA by increased local DNA uptake, protein expression, inflammation, and infiltration of CD3+ T cells. *J Immunol* 2007; **179**: 4741–4753.
29 Alvarez-Lajonchere L, Duenas-Carrera S. Complete definition of immunological correlates of protection and clearance of hepatitis C virus infection: a relevant pending task for vaccine development. *Int Rev Immunol* 2012; **31**: 223–242.
30 Zhou Y, Zhang Y, Yao Z, Moorman JP, Jia Z. Dendritic cell-based immunity and vaccination against hepatitis C virus infection. *Immunology* 2012; **136**: 385–396.
31 Inchauspe G, Feinstone S. Development of a hepatitis C virus vaccine. *Clin Liver Dis* 2003; **7**: 243–259; xi.
32 Li YP, Kang HN, Babiuk LA, Liu Q. Elicitation of strong immune responses by a DNA vaccine expressing a secreted form of hepatitis C virus envelope protein E2 in murine and porcine animal models. *World J Gastroenterol* 2006; **12**: 7126–7135.
33 Meurens F, Summerfield A, Nauwynck H, Saif L, Gerdts V. The pig: a model for human infectious diseases. *Trends Microbiol* 2012; **20**: 50–57.
34 Brennan AJ, Chia J, Browne KA, Ciccone A, Ellis S, Lopez JA *et al.* Protection from endogenous perforin: glycans and the C terminus regulate exocytic trafficking in cytotoxic lymphocytes. *Immunity* 2011; **34**: 879–892.
35 Zarrin AA, Malkin L, Fong I, Luk KD, Ghose A, Berinstein NL. Comparison of CMV, RSV, SV40 viral and Vlambda1 cellular promoters in B and T lymphoid and non-lymphoid cell lines. *Biochim Biophys Acta* 1999; **1446**: 135–139.
36 Wang S, Konorev EA, Kotamraju S, Joseph J, Kalivendi S, Kalyanaraman B. Doxorubicin induces apoptosis in normal and tumor cells via distinctly different mechanisms. intermediacy of H(2)O(2)- and p53-dependent pathways. *J Biol Chem* 2004; **279**: 25535–25543.
37 Zhan Y, van de Water B, Wang Y, Stevens JL. The roles of caspase-3 and bcl-2 in chemically-induced apoptosis but not necrosis of renal epithelial cells. *Oncogene* 1999; **18**: 6505–6512.
38 Fink SL, Cookson BT. Apoptosis, pyroptosis, and necrosis: mechanistic description of dead and dying eukaryotic cells. *Infect Immun* 2005; **73**: 1907–1916.
39 Degterev A, Hitomi J, Germscheid M, Ch'en IL, Korkina O, Teng X *et al.* Identification of RIP1 kinase as a specific cellular target of necrostatins. *Nat Chem Biol* 2008; **4**: 313–321.
40 Ofengeim D, Yuan J. Regulation of RIP1 kinase signalling at the crossroads of inflammation and cell death. *Nat Rev Mol Cell Biol* 2013; **14**: 727–736.
41 Prikhod'ko EA, Prikhod'ko GG, Siegel RM, Thompson P, Major ME, Cohen JI. The NS3 protein of hepatitis C virus induces caspase-8-mediated apoptosis independent of its protease or helicase activities. *Virology* 2004; **329**: 53–67.
42 Krysko O, De Ridder L, Cornelissen M. Phosphatidylserine exposure during early primary necrosis (oncosis) in JB6 cells as evidenced by immunogold labeling technique. *Apoptosis* 2004; **9**: 495–500.
43 Vernon PJ, Tang D. Eat-me: autophagy, phagocytosis, and reactive oxygen species signaling. *Antioxid Redox Signal* 2013; **18**: 677–691.
44 Sawai H, Domae N. Discrimination between primary necrosis and apoptosis by necrostatin-1 in Annexin V-positive/propidium iodide-negative cells. *Biochem Biophys Res Commun* 2011; **411**: 569–573.
45 Kramer G, Erdal H, Mertens HJ, Nap M, Mauermann J, Steiner G *et al.* Differentiation between cell death modes using measurements of different soluble forms of extracellular cytokeratin 18. *Cancer Res* 2004; **64**: 1751–1756.
46 Leers MP, Kolgen W, Bjorklund V, Bergman T, Tribbick G, Persson B *et al.* Immunocytochemical detection and mapping of a cytokeratin 18 neo-epitope exposed during early apoptosis. *J Pathol* 1999; **187**: 567–572.
47 Schutte B, Henfling M, Kolgen W, Bouman M, Meex S, Leers MP *et al.* Keratin 8/18 breakdown and reorganization during apoptosis. *Exp Cell Res* 2004; **297**: 11–26.
48 Mikkelsen M, Holst PJ, Bukh J, Thomsen AR, Christensen JP. Enhanced and sustained CD8+ T cell responses with an adenoviral vector-based hepatitis C virus vaccine encoding NS3 linked to the MHC class II chaperone protein invariant chain. *J Immunol* 2011; **186**: 2355–2364.
49 Yu W, Grubor-Bauk B, Gargett T, Garrod T, Gowans EJ. A novel challenge model to evaluate the efficacy of hepatitis C virus vaccines in mice. *Vaccine* 2014; **32**: 3409–3416.
50 Galluzzi L, Vitale I, Abrams JM, Alnemri ES, Baehrecke EH, Blagosklonny MV *et al.* Molecular definitions of cell death subroutines: recommendations of the Nomenclature Committee on Cell Death. *Cell Death Differ* 2012; **19**: 107–120.
51 Galluzzi L, Bravo-San Pedro JM, Vitale I, Aaronson SA, Abrams JM, Adam D *et al.* Essential versus accessory aspects of cell death: recommendations of the NCCD 2015. *Cell Death Differ 2015* **22**: 58–73.

© 2016 Macmillan Publishers Limited

52 Voskoboinik I, Whisstock JC, Trapani JA. Perforin and granzymes: function, dysfunction and human pathology. *Nat Rev Immunol* 2015; **15**: 388–400.
53 Lopez JA, Susanto O, Jenkins MR, Lukoyanova N, Sutton VR, Law RH *et al.* Perforin forms transient pores on the target cell plasma membrane to facilitate rapid access of granzymes during killer cell attack. *Blood* 2013; **121**: 2659–2668.
54 Liu MA. DNA vaccines: an historical perspective and view to the future. *Immunol Rev* 2011; **239**: 62–84.
55 Garrod TJ, Grubor-Bauk B, Gargett T, Li Y, Miller DS, Yu W *et al.* DNA vaccines encoding membrane-bound or secreted forms of heat shock protein 70 exhibit improved potency. *Eur J Immunol* 2014; **44**: 1992–2002.
56 Morrow MP, Pankhong P, Laddy DJ, Schoenly KA, Yan J, Cisper N *et al.* Comparative ability of IL-12 and IL-28B to regulate Treg populations and enhance adaptive cellular immunity. *Blood* 2009; **113**: 5868–5877.
57 Voskoboinik I, Thia MC, Fletcher J, Ciccone A, Browne K, Smyth MJ *et al.* Calcium-dependent plasma membrane binding and cell lysis by perforin are mediated through its C2 domain: a critical role for aspartate residues 429, 435, 483, and 485 but not 491. *J Biol Chem* 2005; **280**: 8426–8434.
58 Bugarcic A, Taylor JA. Rotavirus nonstructural glycoprotein NSP4 is secreted from the apical surfaces of polarized epithelial cells. *J Virol* 2006; **80**: 12343–12349.
59 Labrinidis A, Diamond P, Martin S, Hay S, Liapis V, Zinonos I *et al.* Apo2L/TRAIL inhibits tumor growth and bone destruction in a murine model of multiple myeloma. *Clin Cancer Res* 2009; **15**: 1998–2009.
60 BG-B Tessa Gargett, Miller D, Garrod T, Yu S, Wesselingh S, Suhrbier A, Gowans Eric J. Increase in DNA vaccine efficacy by virosome and co-expression of a cytolytic protein. *Clin Transl Immunol* 2014; **3**.

© 2016 Macmillan Publishers Limited